

Electroweak measurements at CMS and ATLAS

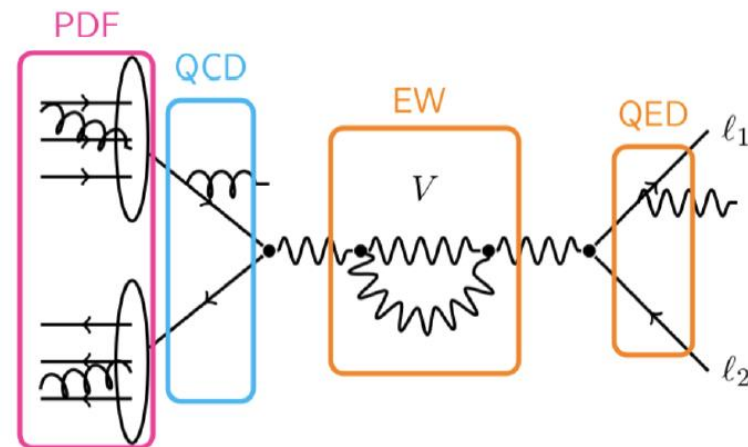
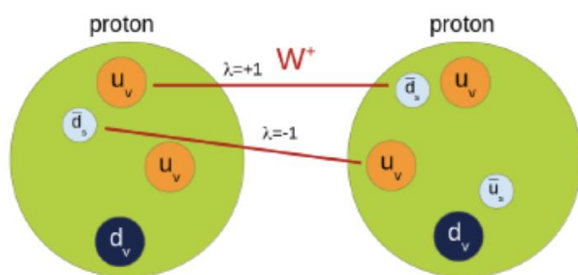
Tairan Xu

23.03.2023

Moriond EW 2023



W/Z measurements



Why the W/Z measurements?

- One of the best understood process in proton collider; cleanest final states
- The Extreme precision is achievable in LHC
 - EWK parameters measurements
 - Probing various QCD effects

ATLAS Wmass Strategy

$$\frac{d\sigma}{dp_1 dp_2} = \left[\frac{d\sigma(m)}{dm} \right] \left[\frac{d\sigma(y)}{dy} \right] \left[\frac{d\sigma(p_T, y)}{dp_T dy} \left(\frac{d\sigma(y)}{dy} \right)^{-1} \right] \left[(1 + \cos^2 \theta) + \sum_{i=0}^7 A_i(p_T, y) P_i(\cos \theta, \phi) \right]$$

Breit-Wigner (under $\frac{d\sigma(m)}{dm}$)
 NNLO pQCD (under $\frac{d\sigma(y)}{dy}$)
 Parton Shower (under $\frac{d\sigma(p_T, y)}{dp_T dy} \left(\frac{d\sigma(y)}{dy} \right)^{-1}$)

Z boson invisible width

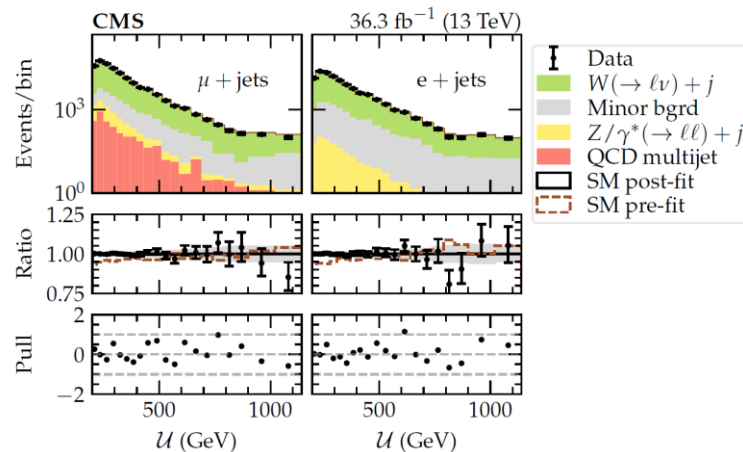


Precision measurement to Z invisible width at 13 TeV: **First Time at a hadron collider!**

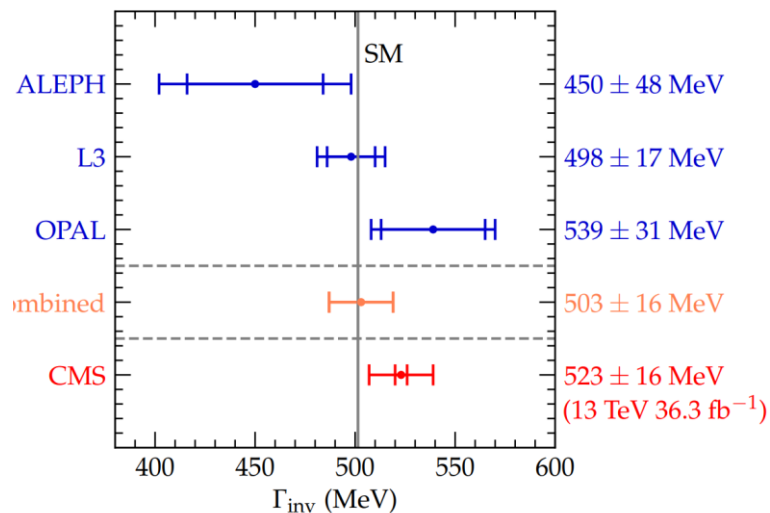
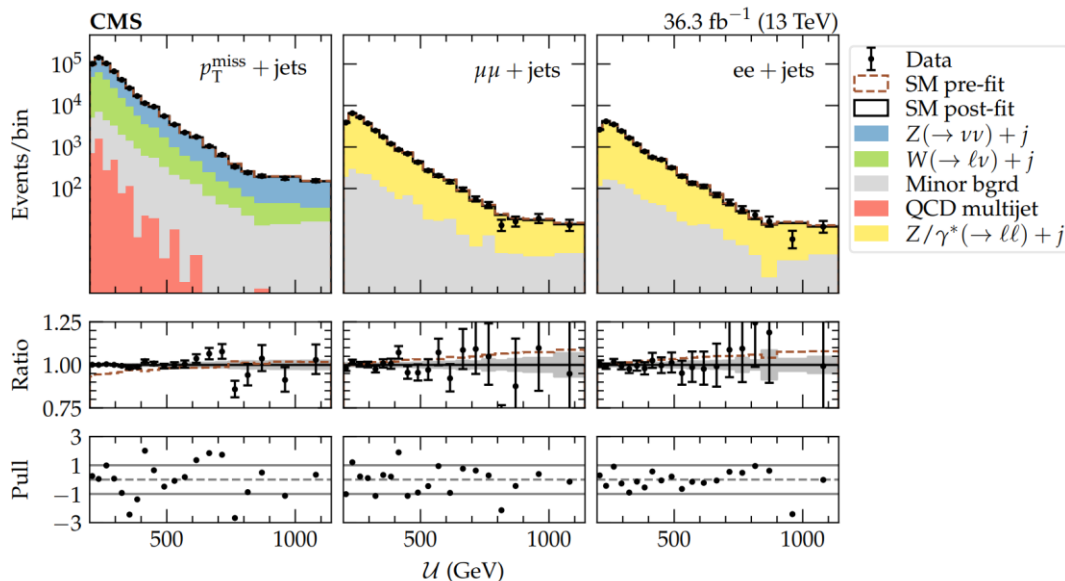
- Z boson decays to particles that are not detected
- constraint on the number of light neutrino species
- reveal non-SM contributions

E_T^{miss}
reconstructed
from calibrated
hadronic recoil
 $u \sim p_T^{W/Z}$

$$\Gamma(Z \rightarrow \nu\bar{\nu}) = \frac{\sigma(Z+jets) \mathcal{B}(Z \rightarrow \nu\bar{\nu})}{\sigma(Z+jets) \mathcal{B}(Z \rightarrow \ell\bar{\ell})} \Gamma(Z \rightarrow \ell\bar{\ell})$$



$$\Gamma_{inv} = 523 \pm 3 \text{ (stat)} \pm 16 \text{ (syst)} \text{ MeV.}$$



τ lepton polarization in Z boson decays

SMP-18-010



$$P_\tau = \frac{1}{\sigma} [\sigma(h_\tau = +1) - \sigma(h_\tau = -1)]$$

$$P_\tau = -A_\tau = -\frac{2v_\tau a_\tau}{v_\tau^2 + a_\tau^2} \approx -2 \cdot \frac{v_\tau}{a_\tau} = -2(1 - 4 \sin^2 \theta_W^{\text{eff}}).$$

Advanced MVA techniques exploited

- [The DeepTau](#) discriminator for τ_h to reject fakes and improve decay mode purity

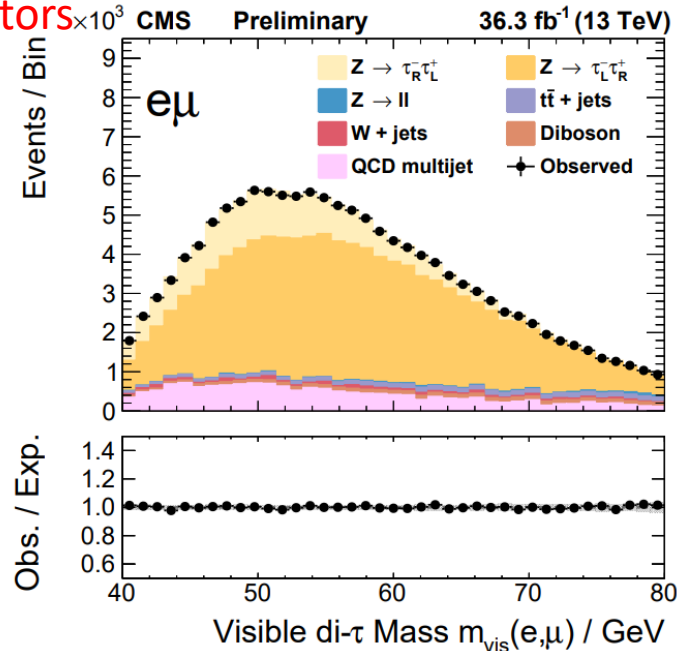
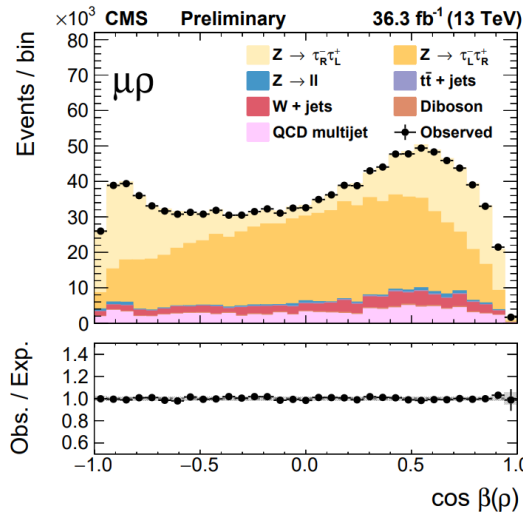
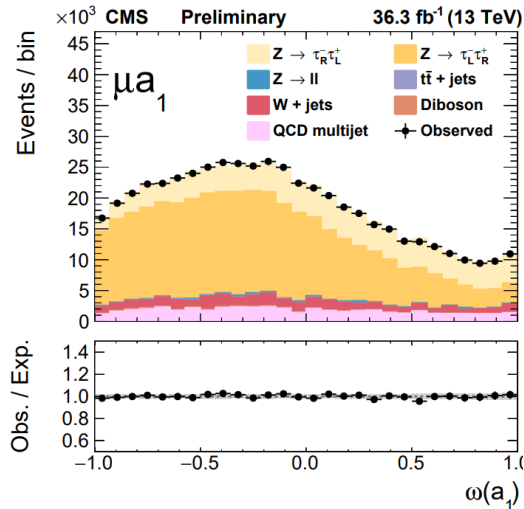
Optimal Observables from previous studies:

$$\omega_h = \cos \zeta_h,$$

$$m_{\text{vis}} = \sqrt{2E_1 E_2 (1 - \cos \angle(\tau_1^{\text{vis}}, \tau_2^{\text{vis}}))}, \text{ polarimetric vectors}$$

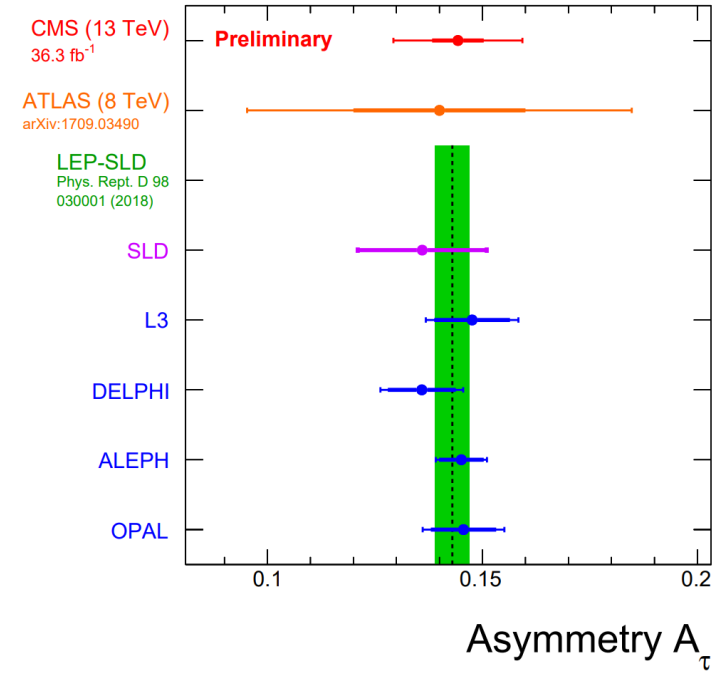
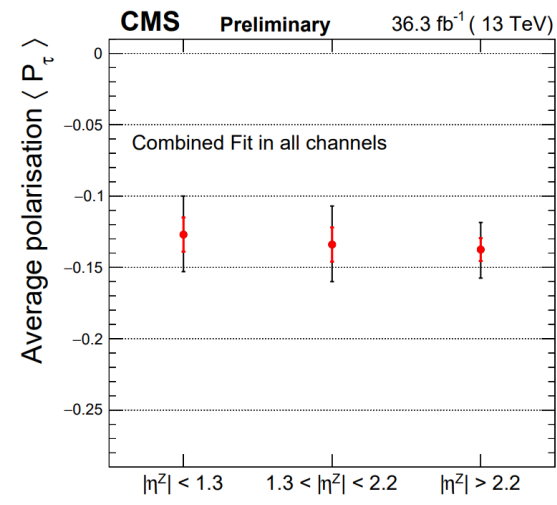
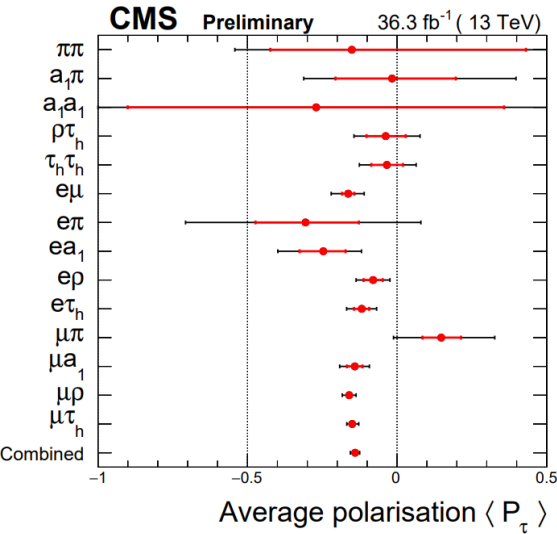
| Final state | Trigger | Lepton selection | Additional selection | |
|-------------------|--|--|--|----------------------------|
| $\tau_h \tau_h$ | τ_h (35 GeV) $\bar{\tau}_h$ (35 GeV) | $p_T^{\tau_h} > 45(40) \text{ GeV}, \eta^{\tau_h} < 2.1$ | Med DeepTau iso | |
| $\tau_\mu \tau_h$ | $\mu(22 \text{ GeV})$ or $\mu(19 \text{ GeV}) \bar{\tau}_h (20 \text{ GeV})$ | $p_T^\mu > 23 \text{ GeV}, \eta^\mu < 2.1$ $p_T^\mu > 20 \text{ GeV}, p_T^{\tau_h} > 30 \text{ GeV}, \eta^{\tau_h} < 2.3$ | $I_{\text{rel}}(\mu) < 0.15$ Med DeepTau iso | $m_T^\mu < 50 \text{ GeV}$ |
| $\tau_e \tau_h$ | $e(25 \text{ GeV})$ | $p_T^e > 30 \text{ GeV}, \eta^e < 2.1$ $p_T^{\tau_h} > 30 \text{ GeV}, \eta^{\tau_h} < 2.3$ | $I_{\text{rel}}(e) < 0.15$ Med DeepTau iso | $m_T^e < 50 \text{ GeV}$ |
| $\tau_e \tau_\mu$ | $\mu(8 \text{ GeV}) e(23 \text{ GeV})$ or $\mu(23 \text{ GeV}) e(12 \text{ GeV})$ | $p_T^e > 15 \text{ GeV}, \eta^e < 2.4$ $p_T^\mu > 15 \text{ GeV}, \eta^\mu < 2.4$ $p_T^\ell > 24 \text{ GeV}$ for lead trigger leg | $I_{\text{rel}}(e) < 0.15$ $I_{\text{rel}}(\mu) < 0.20$ | |

Best-fit templates for different channels



τ lepton polarization in Z boson decays

SMP-18-010



- Systs:**
- Modellings
 - reconstruction
 - background

$$\mathcal{P}_\tau(Z^0) = -0.144 \pm 0.015 = -0.144 \pm 0.006 \text{ (stat)} \pm 0.014 \text{ (syst)}.$$

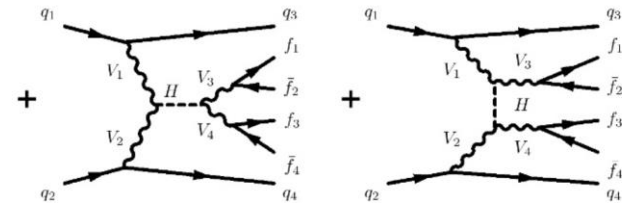
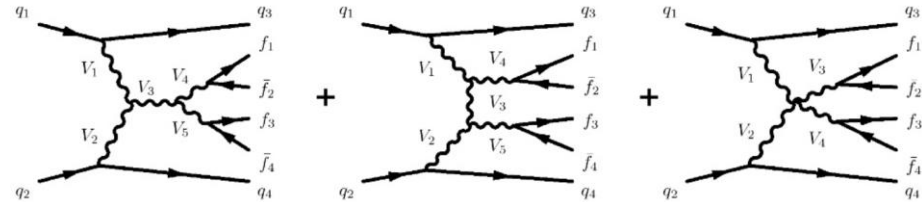
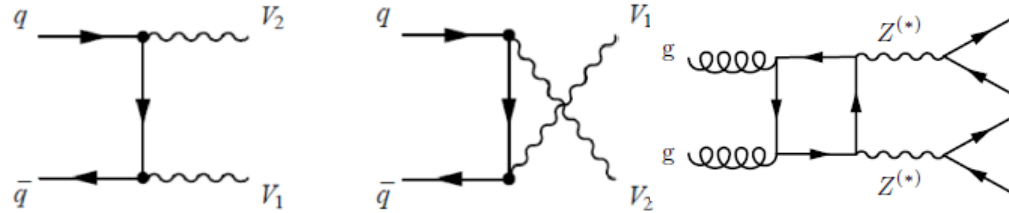
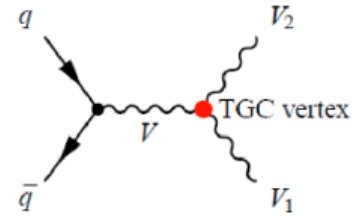
$$\sin^2 \theta_W^{\text{eff}} = 0.2319 \pm 0.0019 = 0.2319 \pm 0.0008 \text{ (stat)} \pm 0.0018 \text{ (syst)}.$$

Spin of τ lepton and spin correlations of τ lepton pairs can be determined and used for BSM search regardless of complicated LHC environment: **new window is open!**

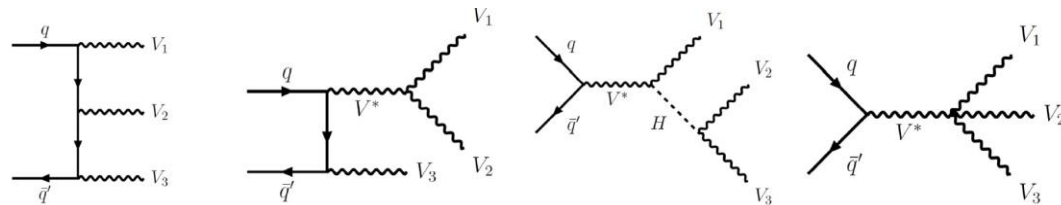
Multi-boson measurements

Test the standard model at TeV scale:

- **Differential cross-section** measurements in validation of current models
- Vector boson scattering/fusion (VBS/F) processes probe the mechanism of **electroweak symmetry breaking**
- Triple/Quartic Gauge Couplings (T/QGC):
 - Search for anomalous couplings
 - Probe new physics



$$\mathcal{L}_{\text{SMEFT}} \approx \mathcal{L}_{\text{SM}}^{(4)} + \sum_i \frac{c_i^{(6)}}{\Lambda^2} \mathcal{O}_i^{(6)} + \sum_j \frac{c_j^{(8)}}{\Lambda^4} \mathcal{O}_j^{(8)}$$



$W^\pm Z$ polarization measurements

CMS: WZ
single boson
polarization
[SMP-20-014](#)

Observation of gauge boson joint-polarization states in $W^\pm Z$ production

- Measured in WZ rest frame: $W_L Z_L$ ($W_0 Z_0$), $W_T Z_L$, $W_L Z_T$, $W_T Z_T$

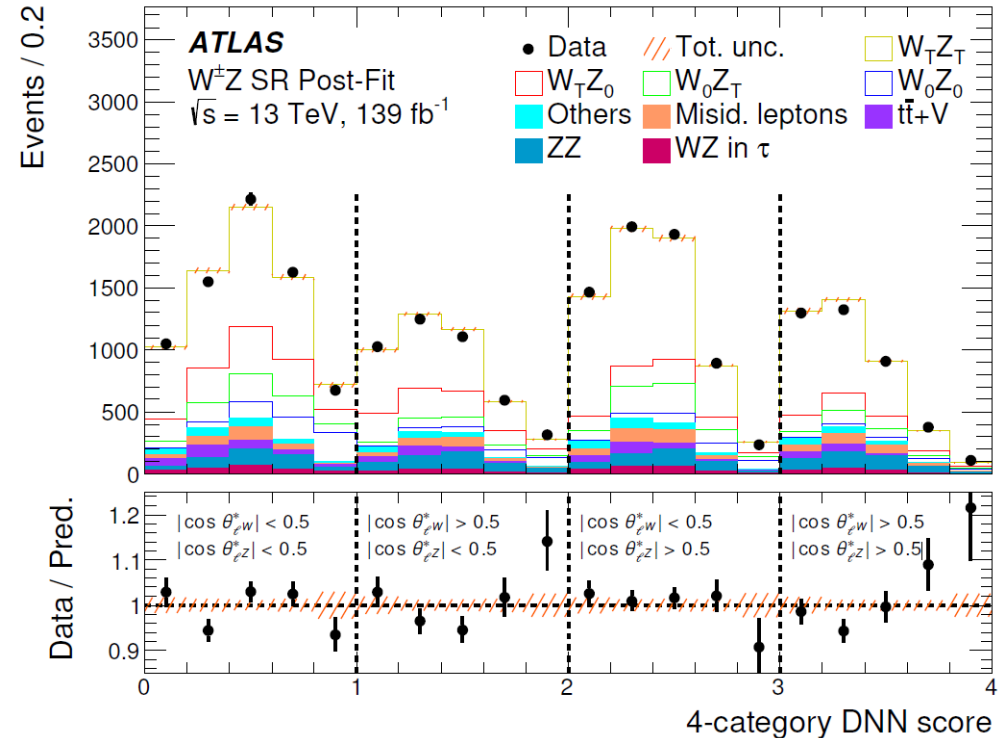
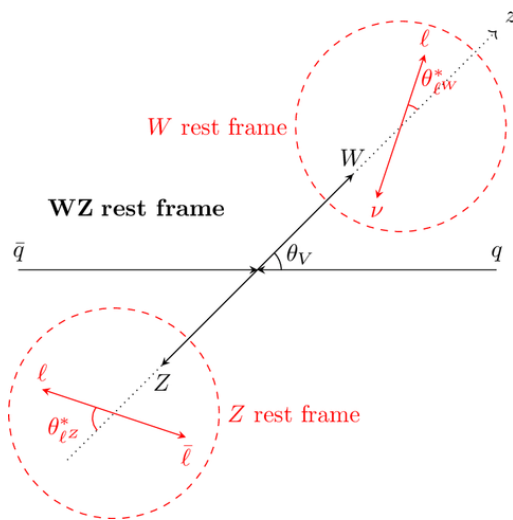
Signal:

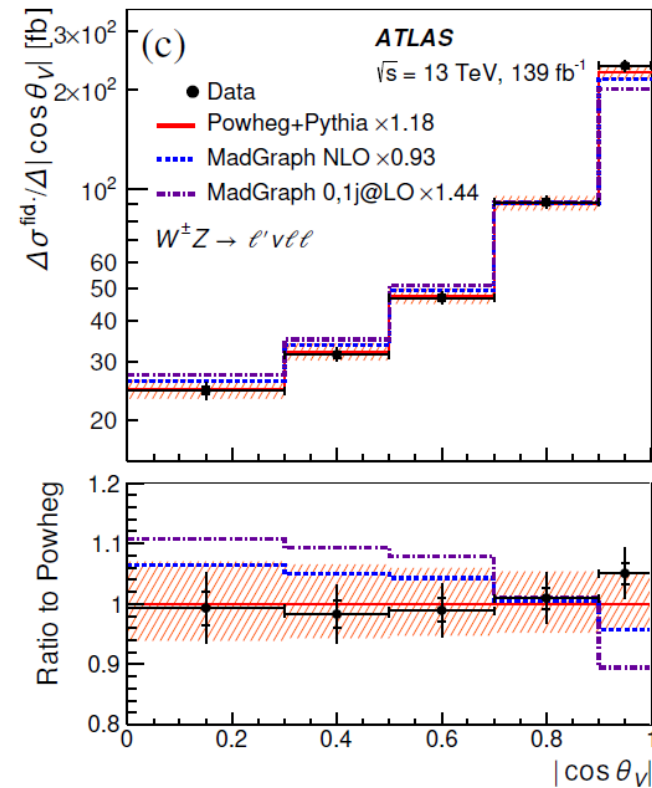
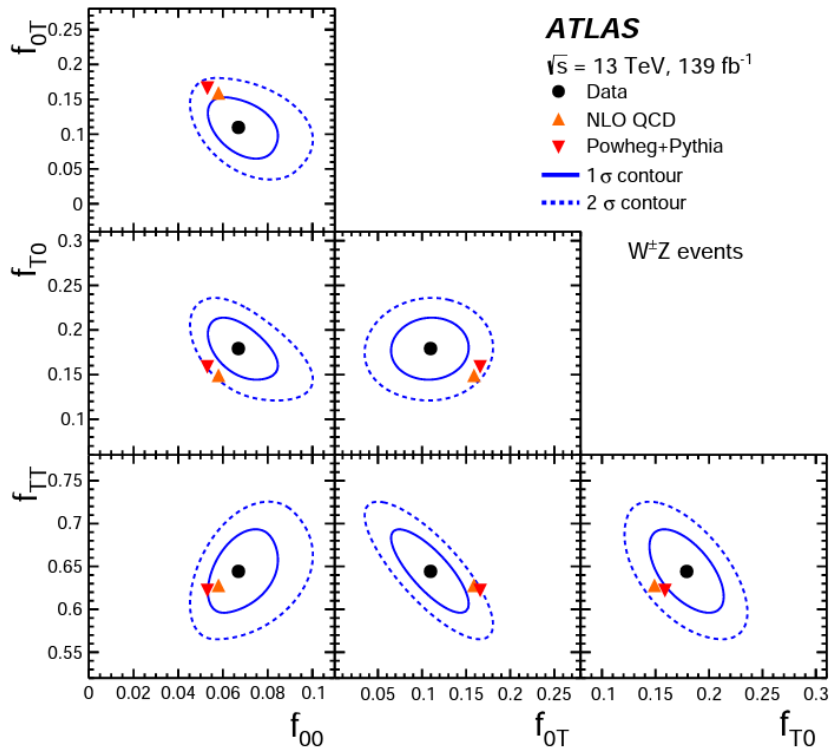
- Polarized WZ with MadGraph @ LO \rightarrow train the DNN model
- Inclusive WZ with Powheg @ NLO + reweighted to polarized states

DNN score as discriminator to separate the polarization states:

$$p_T^{WZ}, p_T^{l^W}, p_T^{l_1^Z}, p_T^{l_2^Z}, E_T^{Miss},$$

$$|y_Z - y_{\ell^W}|, \Delta\phi(\ell^W, \nu), \Delta\phi(\ell_1^Z, \ell_2^Z).$$





- **First Observation** of $W_L Z_L$ state: 7.1 (6.2) σ in observation (expectation)
- Different polarized states are measured and compared to prediction
- Differential cross sections are measured for polarization-sensitive variables.

$$f_{00} = 0.067 \pm 0.010, \quad f_{0T} = 0.110 \pm 0.029, \quad f_{T0} = 0.179 \pm 0.023 \quad \text{and} \quad f_{TT} = 0.644 \pm 0.032$$

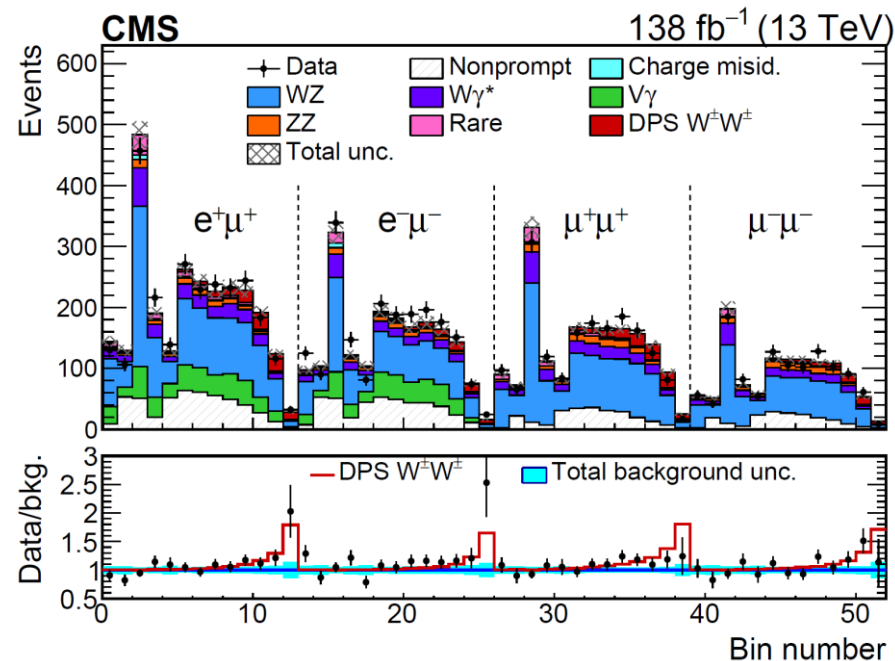


Double parton scattering:

- provides information on the transverse profile of the proton and its energy evolution
- allow the study of correlations among the partons
- Indirect measurement to σ_{eff}

$$\sigma_{AB}^{DPS} = \frac{n}{2} \frac{\sigma_A \sigma_B}{\sigma_{eff}}$$

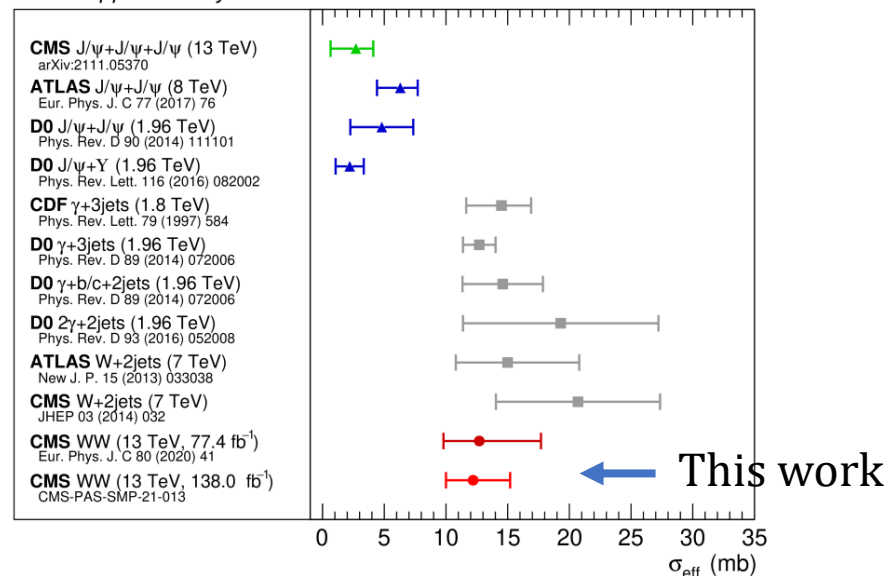
Distinguish backgrounds from signal with BDT



Inclusive Leptonic-decay Xs (6.2 σ observed):

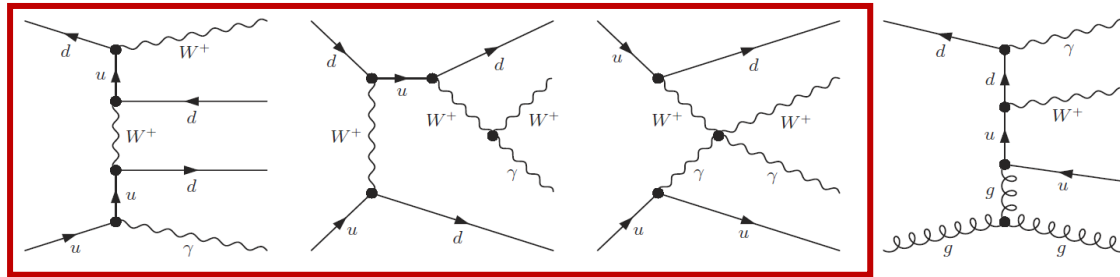
$$80.7 \pm 11.2 \text{ (stat)}_{-8.6}^{+9.5} \text{ (syst)} \pm 12.1 \text{ (model) fb}$$

CMS Supplementary



EWK $W\gamma jj$ measurement

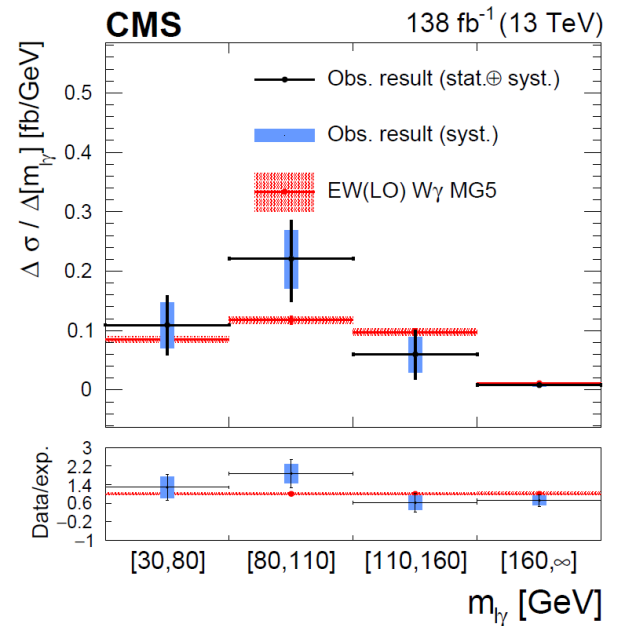
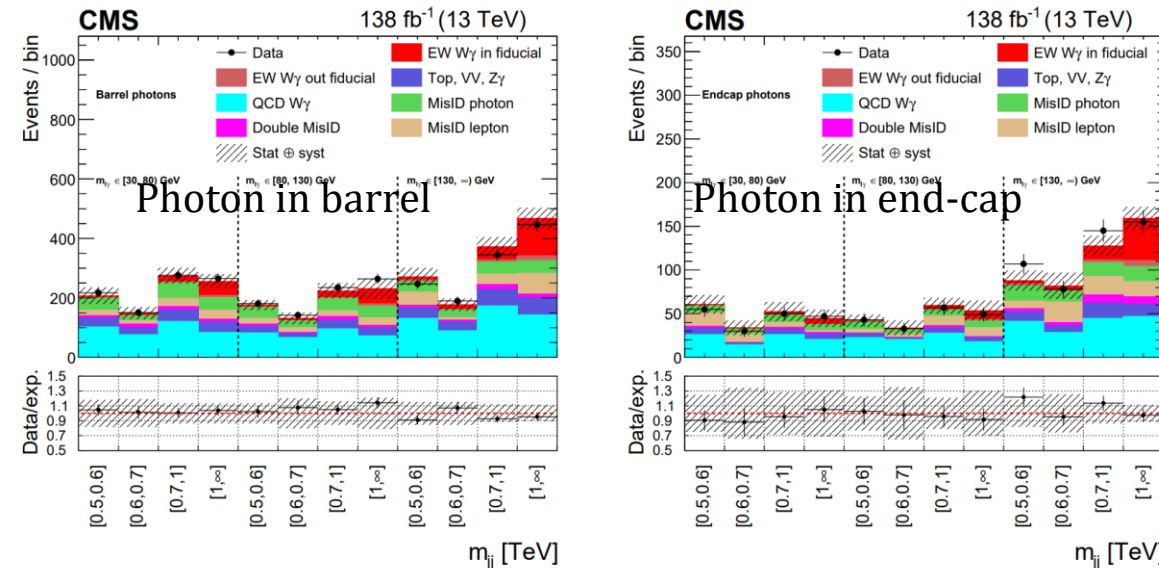
PRD accepted
arXiv:2212.12592



The EWK $W\gamma jj$ production is observed with 6.03σ (6.79σ expected).

Fiducial cross-section and differential cross-section are measured.

$m_{jj}, m_{l\gamma}$ 2D-fit



$$\sigma_{EW}^{\text{fid}} = 23.5 \pm 2.8 \text{ (stat)}_{-1.7}^{+1.9} \text{ (theo)}_{-3.4}^{+3.5} \text{ (syst)} \text{ fb} = 23.5_{-4.7}^{+4.9} \text{ fb.}$$



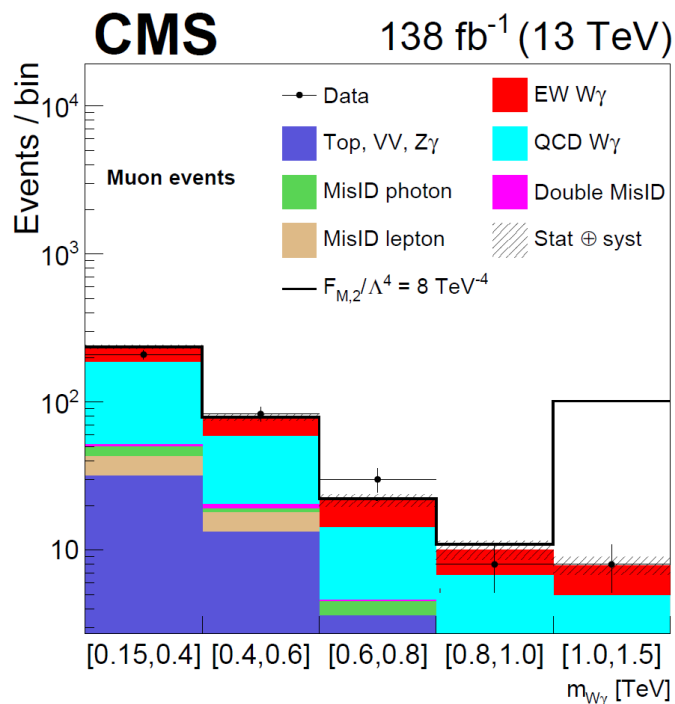
The EWK $W\gamma jj$ production can probe the EFT model via anomalous quartic gauge coupling (aQGC) effect.

Strong constraints are set to EFT dim-8 parameters.

Red rectangle contains the most stringent limits.

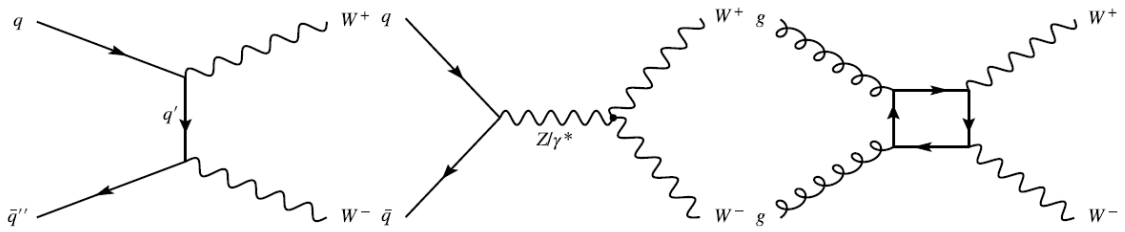
Operators:

- SU(2) strength
- U(1) strength
- Higgs doublet field covariant derivative

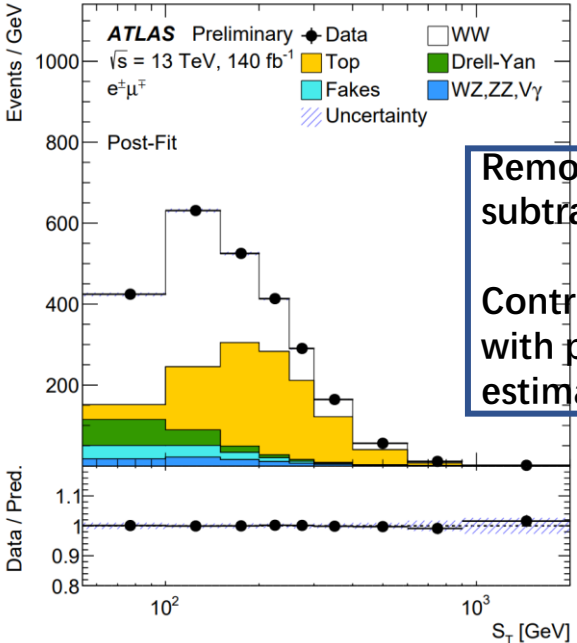
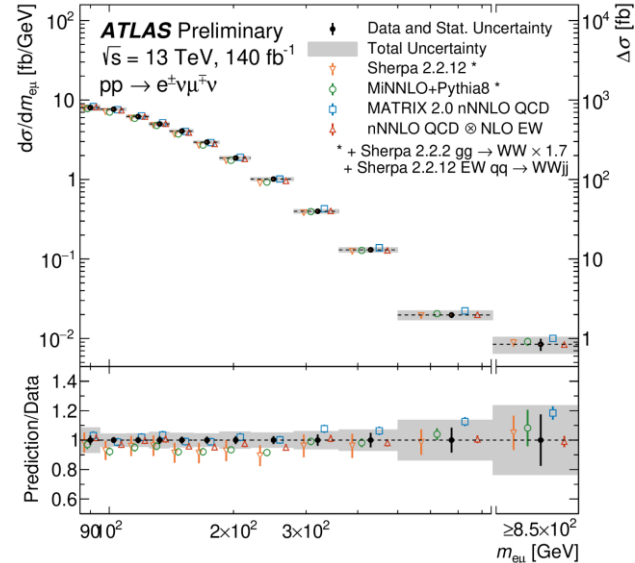


| Expected limit | Observed limit | U_{bound} |
|------------------------------------|------------------------------------|--------------------|
| $-5.1 < f_{M,0}/\Lambda^4 < 5.1$ | $-5.6 < f_{M,0}/\Lambda^4 < 5.5$ | 1.7 |
| $-7.1 < f_{M,1}/\Lambda^4 < 7.4$ | $-7.8 < f_{M,1}/\Lambda^4 < 8.1$ | 2.1 |
| $-1.8 < f_{M,2}/\Lambda^4 < 1.8$ | $-1.9 < f_{M,2}/\Lambda^4 < 1.9$ | 2.0 |
| $-2.5 < f_{M,3}/\Lambda^4 < 2.5$ | $-2.7 < f_{M,3}/\Lambda^4 < 2.7$ | 2.7 |
| $-3.3 < f_{M,4}/\Lambda^4 < 3.3$ | $-3.7 < f_{M,4}/\Lambda^4 < 3.6$ | 2.3 |
| $-3.4 < f_{M,5}/\Lambda^4 < 3.6$ | $-3.9 < f_{M,5}/\Lambda^4 < 3.9$ | 2.7 |
| $-13 < f_{M,7}/\Lambda^4 < 13$ | $-14 < f_{M,7}/\Lambda^4 < 14$ | 2.2 |
| $-0.43 < f_{T,0}/\Lambda^4 < 0.51$ | $-0.47 < f_{T,0}/\Lambda^4 < 0.51$ | 1.9 |
| $-0.27 < f_{T,1}/\Lambda^4 < 0.31$ | $-0.31 < f_{T,1}/\Lambda^4 < 0.34$ | 2.5 |
| $-0.72 < f_{T,2}/\Lambda^4 < 0.92$ | $-0.85 < f_{T,2}/\Lambda^4 < 1.0$ | 2.3 |
| $-0.29 < f_{T,5}/\Lambda^4 < 0.31$ | $-0.31 < f_{T,5}/\Lambda^4 < 0.33$ | 2.6 |
| $-0.23 < f_{T,6}/\Lambda^4 < 0.25$ | $-0.25 < f_{T,6}/\Lambda^4 < 0.27$ | 2.9 |
| $-0.60 < f_{T,7}/\Lambda^4 < 0.68$ | $-0.67 < f_{T,7}/\Lambda^4 < 0.73$ | 3.1 |

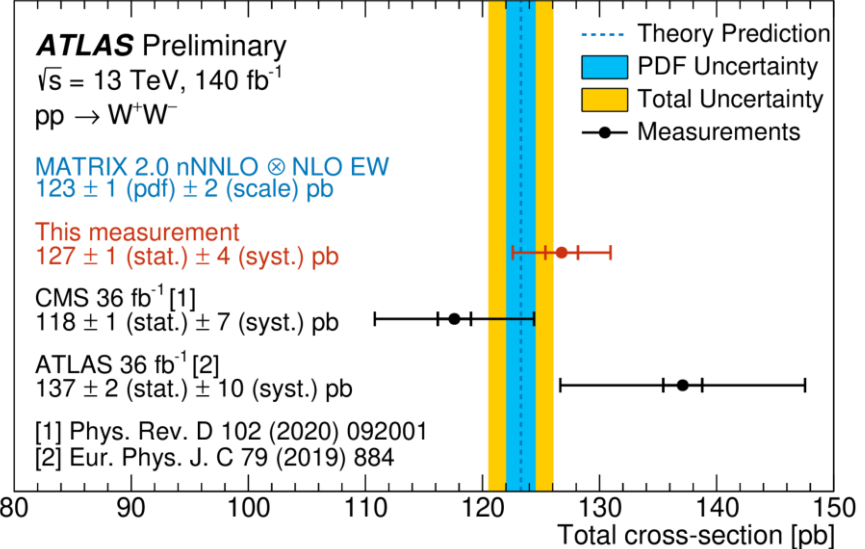
WW inclusive measurement



Incl & Diff cross-section measured.
Most precise result at 13 TeV.



Remove the jet veto to subtract uncertainty.
Control Top background with precise differential estimate of jet CRs.



$W\gamma\gamma/WZ\gamma$ observation

$WZ\gamma$: [ATLAS-CONF-2023-014](#)

$W\gamma\gamma$: [ATLAS-CONF-2023-005](#)

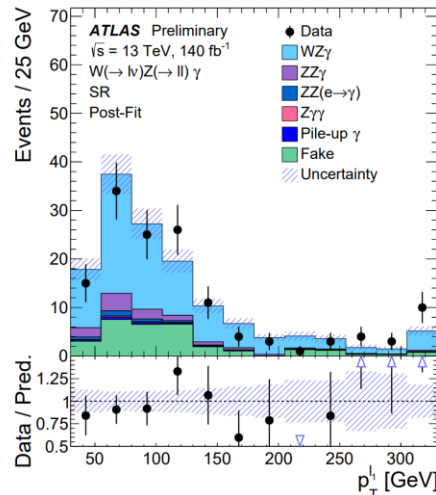
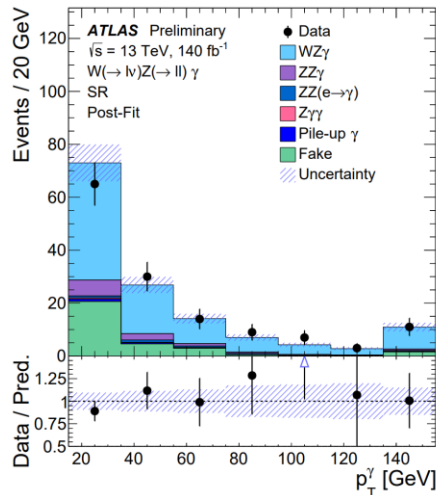
$WZ\gamma$ observation

Simultaneous fit with $\mu_{ZZ\gamma}, \mu_{ZZ}$;

$WZ\gamma$ observed with 6.3σ

$$\sigma_{WZ\gamma} = 2.01 \pm 0.30 \text{ (stat.)} \pm 0.16 \text{ (syst.) fb}$$

| Process | SR | $ZZ\gamma$ CR | $ZZ(e \rightarrow \gamma)$ CR |
|----------------------------|-----------------|-------------------|-------------------------------|
| $WZ\gamma$ | 92 ± 15 | 0.21 ± 0.07 | 0.56 ± 0.14 |
| $ZZ\gamma$ | 10.7 ± 2.3 | 23 ± 5 | 1.8 ± 0.4 |
| $ZZ(e \rightarrow \gamma)$ | 3.0 ± 0.6 | 0.028 ± 0.020 | 30 ± 6 |
| $Z\gamma\gamma$ | 1.05 ± 0.32 | 0.15 ± 0.06 | 0.29 ± 0.10 |
| Fake background | 30 ± 6 | - | - |
| Pile-up γ | 1.9 ± 0.7 | - | - |
| Total predicted | 139 ± 12 | 23 ± 5 | 33 ± 6 |
| Data | 139 | 23 | 33 |



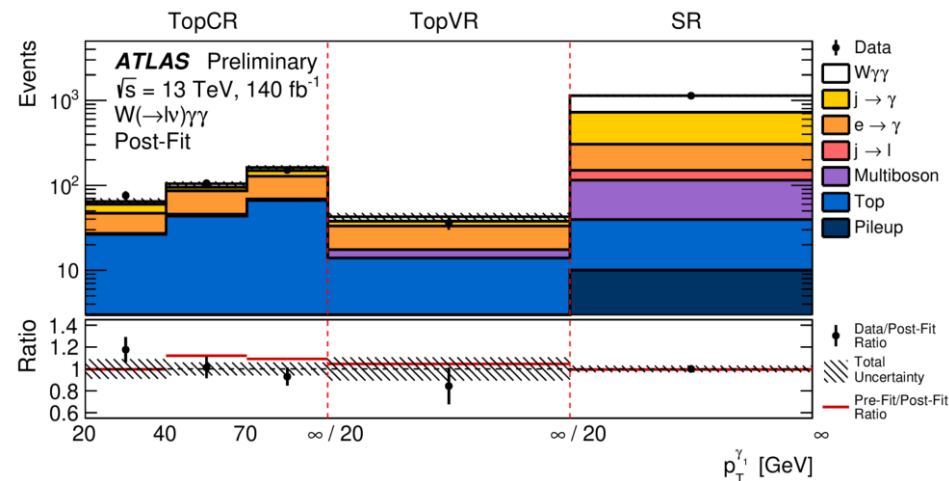
$W\gamma\gamma$ observation

data-driven Fake estimated in control regions

$WZ\gamma$ observed with 5.6σ

$$\sigma_{fid} = 12.1^{+2.5}_{-2.2} \text{ fb}^{-1}$$

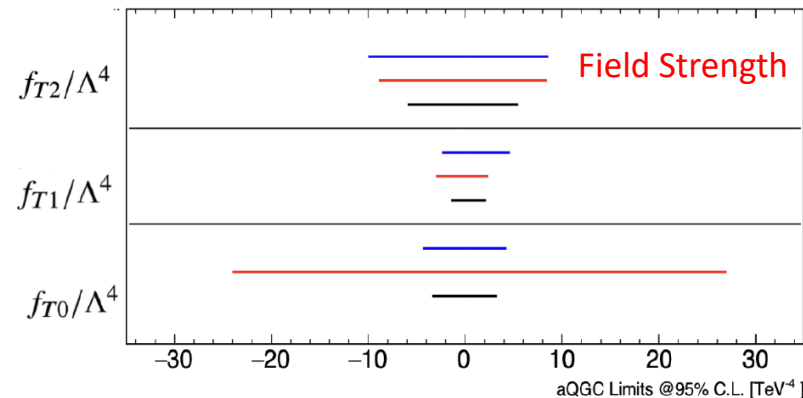
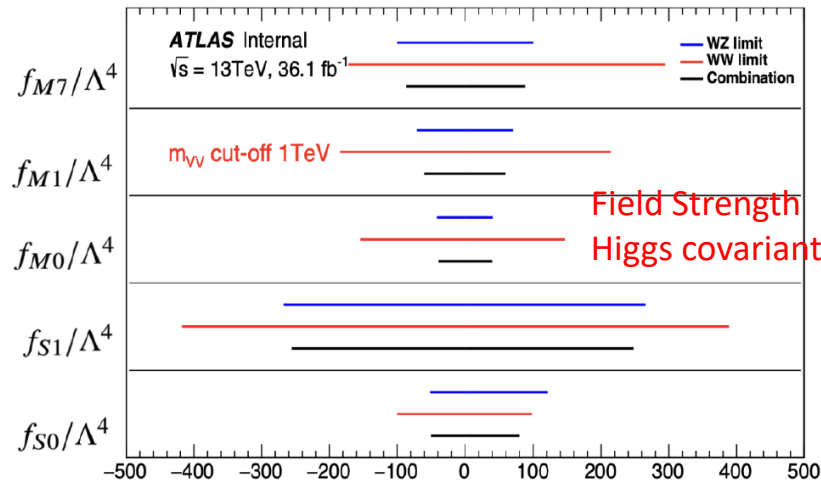
| | SR | TopCR |
|--|-----------------|---------------|
| $W\gamma\gamma$ | 410 ± 60 | 28 ± 5 |
| Non-prompt $j \rightarrow \gamma$ | 420 ± 50 | 42 ± 20 |
| Misidentified $e \rightarrow \gamma$ | 155 ± 11 | 120 ± 9 |
| Multiboson ($WH(\gamma\gamma), WW\gamma, Z\gamma\gamma$) | 76 ± 13 | 5.2 ± 1.7 |
| Non-prompt $j \rightarrow \ell$ | 35 ± 10 | - |
| Top ($t\bar{t}\gamma, tW\gamma, tq\gamma$) | 30 ± 7 | 136 ± 32 |
| Pileup | 10 ± 5 | - |
| Total | $1\ 136 \pm 34$ | 332 ± 18 |
| Data | 1 136 | 333 |



EFT interpretation

$WZjj$ and $W^\pm W^\pm jj$ combination using 2015+2016 data: [ATL-PHYS-PUB-2023-002](#)

- Dim-8 EFT operators are constrained



First ATLAS EFT global Fit: [ATL-PHYS-PUB-2022-037](#)

SMEFT interpretation constraining dim-6 operators with :

- ATLAS Higgs boson data
- ATLAS electroweak data: di-boson, Z boson
- EW precision observables (EWPO) at LEP and SLC.

| Decay channel | Target Production Modes | \mathcal{L} [fb ⁻¹] |
|------------------------------|---|-----------------------------------|
| $H \rightarrow \gamma\gamma$ | ggF, VBF, WH , ZH , $t\bar{t}H$, tH | 139 |
| $H \rightarrow ZZ^*$ | ggF, VBF, WH , ZH , $t\bar{t}H(4\ell)$ | 139 |
| $H \rightarrow WW^*$ | ggF, VBF | 139 |
| $H \rightarrow \tau\tau$ | ggF, VBF, WH , ZH , $t\bar{t}H(\tau_{\text{had}}\tau_{\text{had}})$ | 139 |
| | WH, ZH | 139 |
| $H \rightarrow b\bar{b}$ | VBF | 126 |
| | $t\bar{t}H$ | 139 |

| Process | Important phase space requirements | Observable | \mathcal{L} [fb ⁻¹] |
|--|---|------------------------------------|-----------------------------------|
| $pp \rightarrow e^\pm \nu \mu^\mp \nu$ | $m_{\ell\ell} > 55$ GeV, $p_{\text{T}}^{\text{jet}} < 35$ GeV | $p_{\text{T}}^{\text{lead. lep.}}$ | 36 |
| $pp \rightarrow \ell^\pm \nu \ell^+ \ell^-$ | $m_{\ell\ell} \in (81, 101)$ GeV | m_{T}^{WZ} | 36 |
| $pp \rightarrow \ell^+ \ell^- \ell^+ \ell^-$ | $m_{4\ell} > 180$ GeV | m_{Z2} | 139 |
| $pp \rightarrow \ell^+ \ell^- jj$ | $m_{jj} > 1000$ GeV, $m_{\ell\ell} \in (81, 101)$ GeV | $\Delta\phi_{jj}$ | 139 |

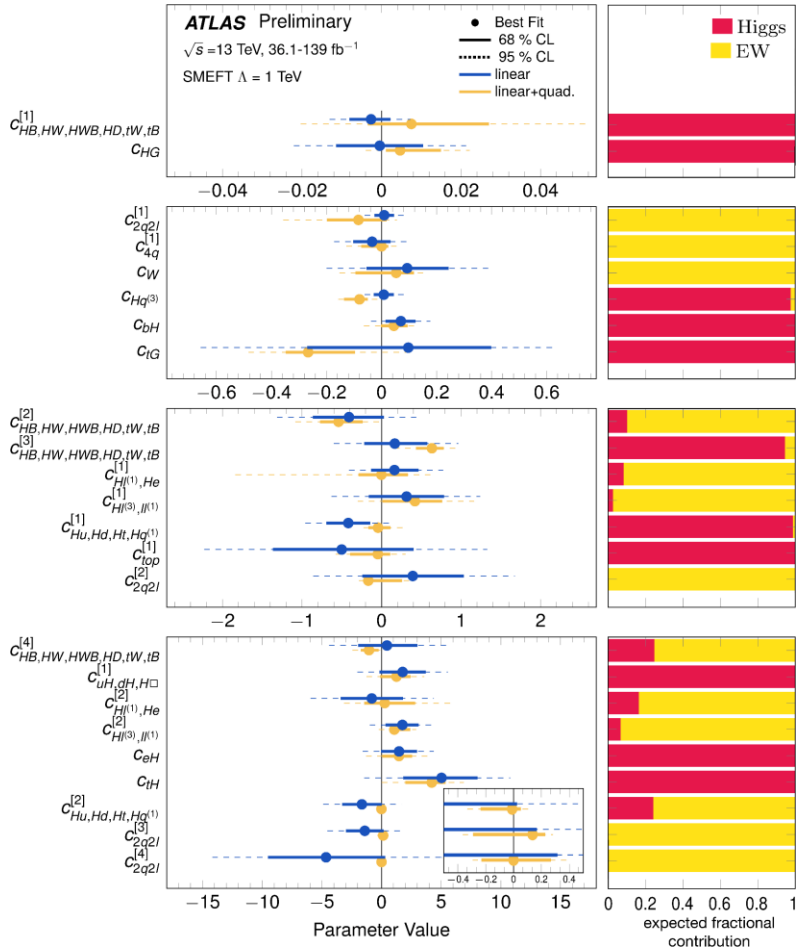
$$\Gamma_Z, \sigma_{\text{had}}^0, R_\ell^0, \bar{A}_{\text{FB}}^{0, \ell^-}, R_b^0, R_c^0, A_{\text{FB}}^{0, b}, \text{ and } A_{\text{FB}}^{0, c}$$



ATLAS only

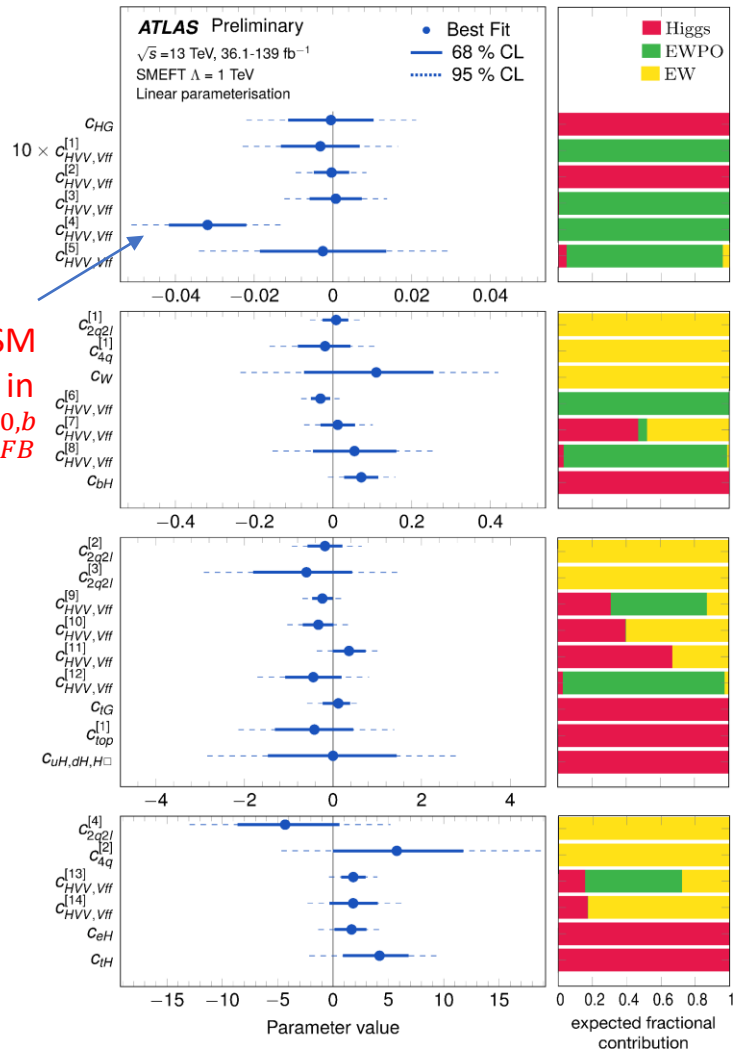
linear combinations of wilson coefficients

ATLAS + EWPO



linear+quad provided as an insight of the impact of higher order terms

From SM excess in $A_{FB}^{0,c}, A_{FB}^{0,b}$



A SMEFT framework is built to include additional results straightforward.

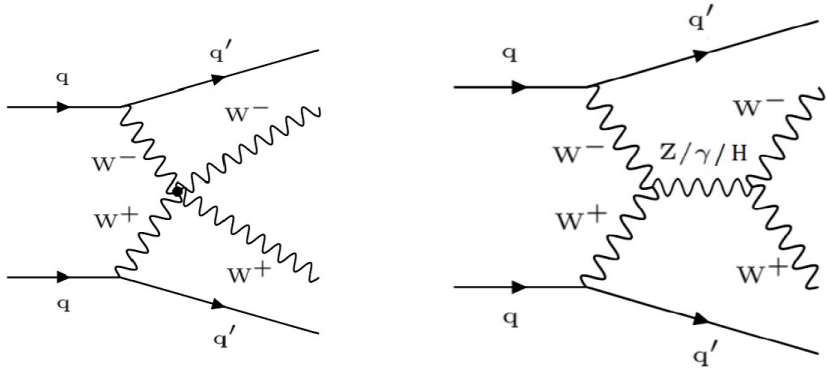
Summary

- New single- and multi-boson measurements at the LHC
 - Precision measurement of the Z boson invisible width
 - Measurement of the τ lepton polarization in Z boson decays
 - Polarization measurements in EWK WZ process
 - Azimuthal correlations in Z+jets events (backup)
- Observation of several rare multi-boson production processes:
 - $W^\pm W^\pm$ double parton scattering at CMS
 - $W^+ W^- jj$ process at CMS
 - $W^+ W^- jj$ at CMS (backup)
 - $W\gamma\gamma$ at ATLAS
 - $WZ\gamma$ at ATLAS
 - EW $Z(\rightarrow \nu\nu)\gamma jj$ with high p_T^γ process in at ATLAS (backup)
- New & Strong constraints on New Physics (EFT):
 - Including new rare processes;
 - Combinations

Challenges and opportunities ahead with more data and higher quality !

Backup

Observation of W^+W^-jj production



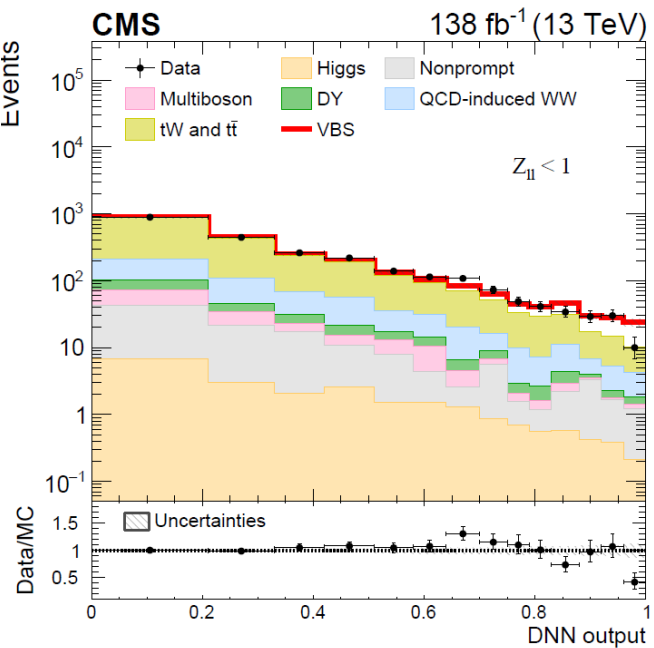
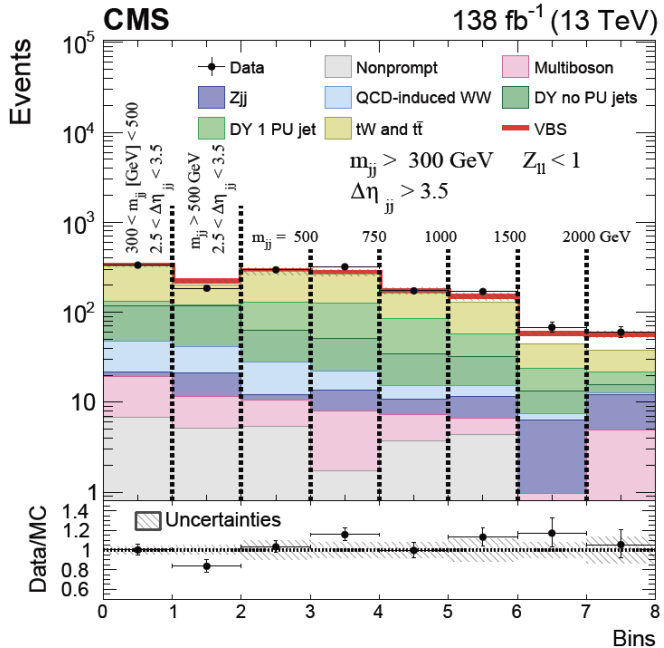
Vector boson scattering measurement:

- Probe the nature of Higgs sector
- Search for BSM effects

DNN exploited to increase the sensitivity

- Large $\Delta\eta_{jj}$, m_{jj} , small Zeppenfeld

$$Z_{lll2} = \frac{1}{2} \left| \left(\eta_{l1} - \frac{1}{2}(\eta_{j1} + \eta_{j1}) \right) + \left(\eta_{l1} - \frac{1}{2}(\eta_{j1} + \eta_{j1}) \right) \right|$$



Results:

- Observed (expected) with 5.6 (5.2) σ
- Fiducial cross-section measured 10.2 ± 2.0 fb (9.1 ± 0.6 fb expected)

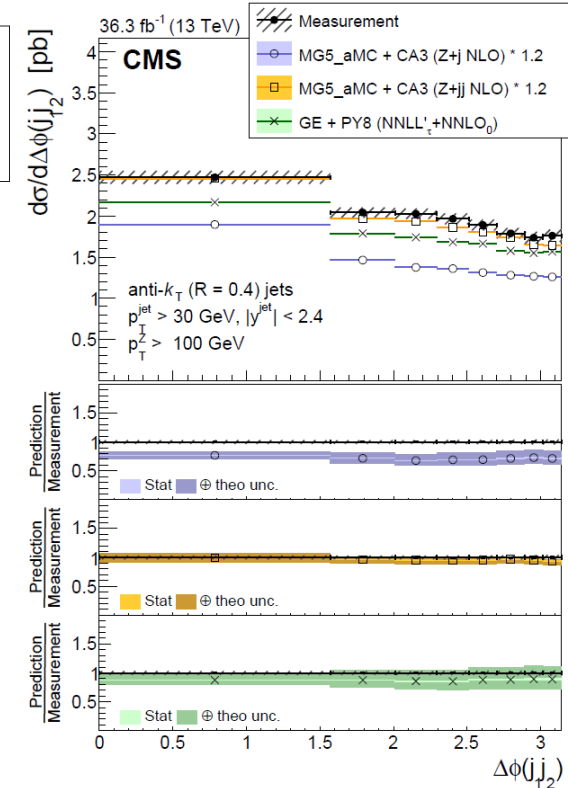
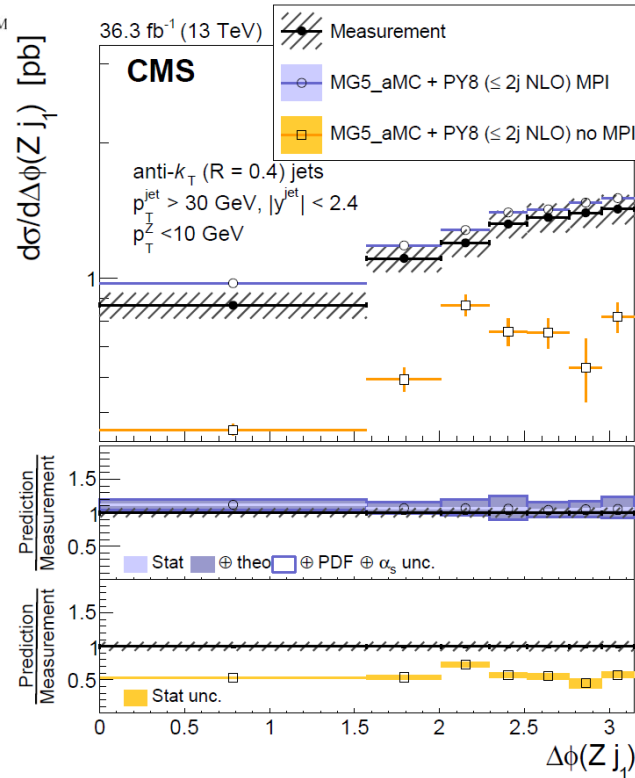
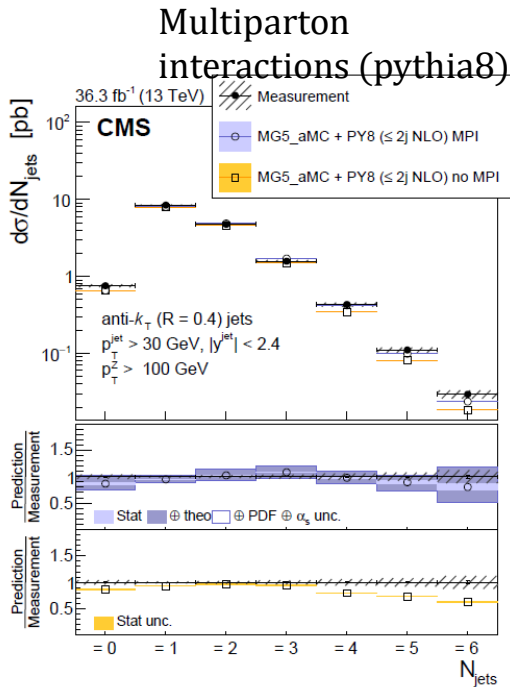


Measurement to the azimuthal correlation $\Delta\phi$ between Z and leading jet, and two leading jets in p_T^Z categories; compared to various theoretical predictions.

- Hard partonic radiation increases in high p_T^Z : probe QCD effects
- To study the NLO production with PS and hadronization as well as jet multiplicity

| Generator | PDF | Matrix element | Tune |
|--------------------------------------|------------------------|------------------------------------|---------------|
| MG5_AMC+Py8 ($\leq 2j$ NLO) [37] | NNPDF3.0 (NLO) [43] | NLO ($2 \rightarrow Z+0,1,2$) | CUETP8M1 [44] |
| MG5_AMC+Py8 ($\leq 4j$ LO) [37,53] | NNPDF2.3 (LO) [48] | LO ($2 \rightarrow Z+0,1,2,3,4$) | CUETP8M1 [44] |
| MG5_AMC+CA3 (Z+1 NLO) [37] | PB NLO set2 (NLO) [20] | NLO ($2 \rightarrow Z+1$) | — |
| MG5_AMC+CA3 (Z+2 NLO) [37] | PB NLO set2 (NLO) [20] | NLO ($2 \rightarrow Z+2$) | — |
| MG5_AMC+CA3 (Z $\leq 3j$ LO) [37,51] | PB NLO set2 (NLO) [20] | LO ($2 \rightarrow Z+0,1,2,3$) | — |
| GENEVA (Z+0 NNLO) [22+25] | NNPDF3.1 (NLO) [54] | NNLO ($2 \rightarrow Z$) | CUETP8M |

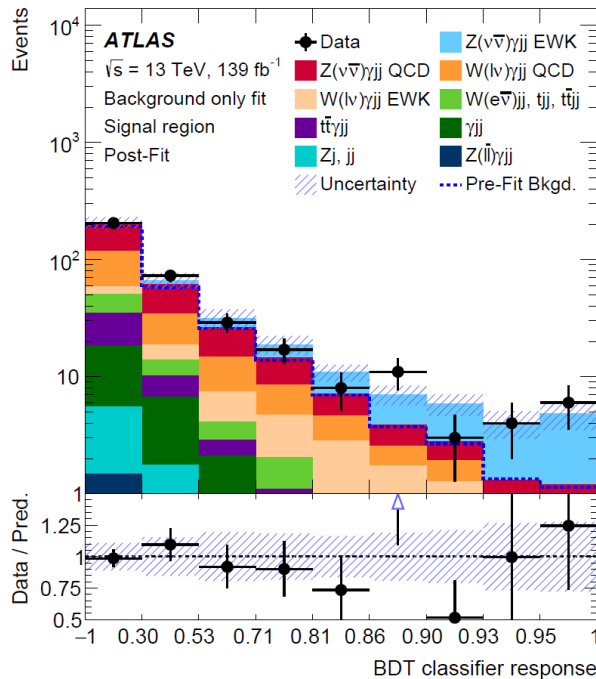
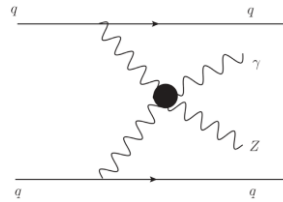
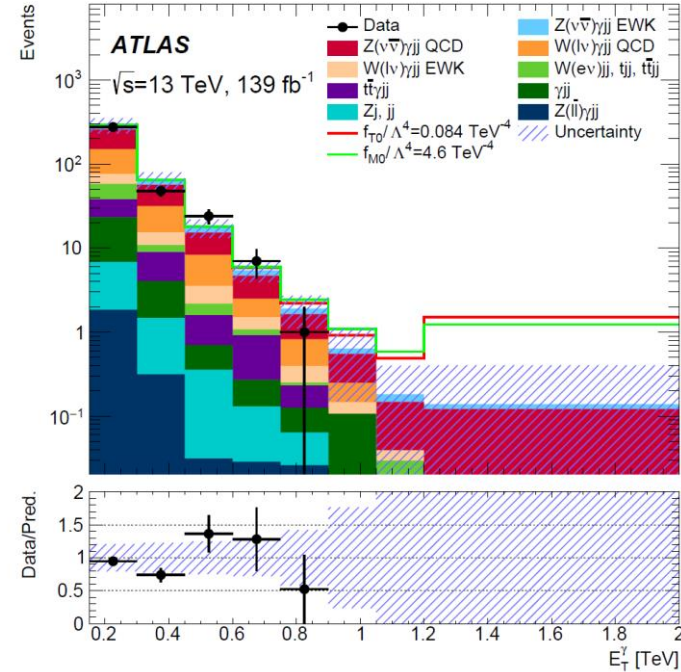
Measured in p_T^Z [0, 10],[30,50],[100,] categories



EW $Z(\rightarrow \nu\nu)\gamma jj$

- Previous observation at 5.2σ in ATLAS: [Eur. Phys. J. C 82 \(2022\) 105](#)
- New measurement with extra $p_T^\gamma > 150 \text{ GeV}$ requirement to enrich the QGC events:
 - observed (expected): 3.2σ (3.7σ)

BDT to separate signal from backgrounds



| Coefficient | E_c [TeV] | Observed limit [TeV ⁻⁴] | Expected limit [TeV ⁻⁴] |
|--------------------|-------------|-------------------------------------|-------------------------------------|
| f_{T0}/Λ^4 | 1.7 | $[-8.7, 7.1] \times 10^{-1}$ | $[-8.9, 7.3] \times 10^{-1}$ |
| f_{T5}/Λ^4 | 2.4 | $[-3.4, 4.2] \times 10^{-1}$ | $[-3.5, 4.3] \times 10^{-1}$ |
| f_{T8}/Λ^4 | 1.7 | $[-5.2, 5.2] \times 10^{-1}$ | $[-5.3, 5.3] \times 10^{-1}$ |
| f_{T9}/Λ^4 | 1.9 | $[-7.9, 7.9] \times 10^{-1}$ | $[-8.1, 8.1] \times 10^{-1}$ |
| f_{M0}/Λ^4 | 0.7 | $[-1.6, 1.6] \times 10^2$ | $[-1.5, 1.5] \times 10^2$ |
| f_{M1}/Λ^4 | 1.0 | $[-1.6, 1.5] \times 10^2$ | $[-1.4, 1.4] \times 10^2$ |
| f_{M2}/Λ^4 | 1.0 | $[-3.3, 3.2] \times 10^1$ | $[-3.0, 3.0] \times 10^1$ |